

Beneficial effects of annealing on amorphous Nb–Si thin-film thermometers

D. Querlioz, E. Helgren, D. R. Queen, and F. Hellman^{a)}
 Department of Physics, University of California, Berkeley, California 94720

R. Islam and David. J. Smith
 Center for Solid State Science, Department of Physics and Astronomy, Arizona State University,
 Tempe, Arizona 85287

(Received 26 July 2005; accepted 27 September 2005; published online 21 November 2005)

Amorphous Nb–Si alloys have a temperature-dependent resistivity which can be tuned over many decades by controlling composition and are used for thin-film thermometers. Annealing at temperatures from 100 to 500 °C produces dramatic but easily controlled increases in resistivity, both magnitude and temperature dependence, for insulating and metallic samples with compositions ranging from 8–15 at. %Nb. A transition from metal to insulator is induced by annealing an initially metallic sample. Annealing produces thermal stability against subsequent heat treatment, allowing annealed films to be used as low-temperature thermometers even when they are cycled to temperatures as high as 500 °C. Cross-section transmission electron microscopy and energy-dispersive x-ray analysis show that the initially amorphous films develop Nb-rich clusters within an amorphous Nb-depleted matrix, explaining the observed resistivity increase. © 2005 American Institute of Physics. [DOI: 10.1063/1.2135380]

Amorphous Nb–Si alloys ($a\text{-Nb}_x\text{Si}_{1-x}$) alloys exhibit a wide range of resistivity versus temperature $\rho(T)$, with a $T=0$ metal-insulator transition (MIT) for $x=0.115$.^{1–4} Both the magnitude of ρ and its derivative $d\rho/dT$ depend strongly on x . Alloys on the metallic side of the MIT have finite resistivity ρ (and finite conductivity $\sigma=1/\rho$) in the limit as T approaches 0, with σ near the MIT given by $\sigma=\sigma_0+AT^{1/2}+BT$. Alloys on the insulating side have infinite resistivity $\rho(\sigma=0)$ in the limit as T approaches 0, with σ best fit by $\sigma=\sigma_0\exp(T/T_0)^{-1/2}$. Amorphous Nb–Si is relatively easily prepared by vapor deposition techniques, making it an excellent choice for a thin-film thermometer in microchip applications. $a\text{-Nb–Si}$ and related $a\text{-Si}$ or Ge alloys are generally used for low-temperature applications,^{5–7} but are also used for measurements up to room temperature.^{8–10} Their use is, however, limited by thermal instability if exposed to temperatures above room temperature, which cause irreversible changes in their $\rho(T)$ calibration. (Note, for example, that the related material $a\text{-Au–Ge}$ must be stored at LN₂ temperature to avoid decay of properties.)¹⁰ This instability is a serious technical problem, even when the only objective is their use as a low-temperature thermometer, because it limits the temperature range to which microchips with $a\text{-Nb–Si}$ thermometers can be exposed. In this letter, we characterize and explain this annealing phenomenon, and show that it can be eliminated by a suitable annealing pretreatment. We also show that resistivity can be controlled by annealing, which is significantly easier to accomplish than high precision composition control.

In the present work, $a\text{-Nb}_x\text{Si}_{1-x}$ films were grown by magnetron co-sputtering onto Si substrates coated with $a\text{-Si–N}$. Film thicknesses were approximately 500 Å, measured by low-angle x-ray diffraction. Compositions were measured for several samples by Rutherford backscattering; values obtained were comparable to literature values for samples of similar ρ .^{1–3} $\rho(T)$ was measured from 4.2 K to room temperature using a four-wire measurement technique.

Samples were annealed using a rapid thermal annealing (RTA) system in flowing forming gas (5% H₂ in N₂ gas, used to capture O₂). The annealing time was a few minutes, and was shown not to have a significant influence (discussed below). A typical annealing profile was 30 s to reach the desired temperature, followed by 2 min at temperature, after which the heater was turned off and the temperature relaxed approximately exponentially to room temperature (~5 min to reach 50 °C). Temperature during annealing was measured with a thermocouple inserted inside the sample plate. Error bars on ρ and T are ~5%.

Figure 1 shows $\rho(T)$ plotted on a logarithmic scale for a sample on the insulating side of the MIT (~8 at. % Nb) in the unannealed state, and after various anneals. The inset shows conductivity $\sigma(T)=1/\rho(T)$ versus T , to show the $T\rightarrow 0$ insulating nature of this sample. Annealing has no effect at 100 °C, and little effect at 200 °C. With higher annealing temperatures, ρ increases and is more strongly temperature dependent. High-temperature annealing causes enormous changes (e.g., 10⁵ change in ρ at 4.2 K by annealing at 500 °C). A usual figure of merit (FOM) for thermometry is $(1/\rho)d\rho/dT=(1/R)dR/dT$; a large change in signal for a given change in temperature requires large dR/dT and small R due to I^2R heating which limits the useable current. A better FOM is $(T/\rho)d\rho/dT$ since typically the temperature change to be resolved is smaller at lower T , i.e., fractional change in temperature $\Delta T/T$. Figure 1(b) shows a steady increase in the FOM upon annealing. Figure 1(b) also shows the increase in FOM with decreasing at. % Nb; this is not always useful due to the awkwardness of working with large ρ . The FOM is nearly independent of T , demonstrating the value of these semiconducting thermometers at low T .

Annealing has similar effects on metallic samples but the magnitude of the induced change is smaller. Resistivity is shown in Fig. 2(a) for a 13 at. % Nb sample; the inset shows σ at lower T as a function of $T^{1/2}$. As with many disordered metals, $a\text{-NbSi}$ shows $T^{1/2}$ behavior for σ at low T where conduction is dominated by the precursor to the Coulomb gap.^{1,2,4} The inset of Fig. 2 shows that the unannealed sample

^{a)}Electronic mail: fhellman@berkeley.edu

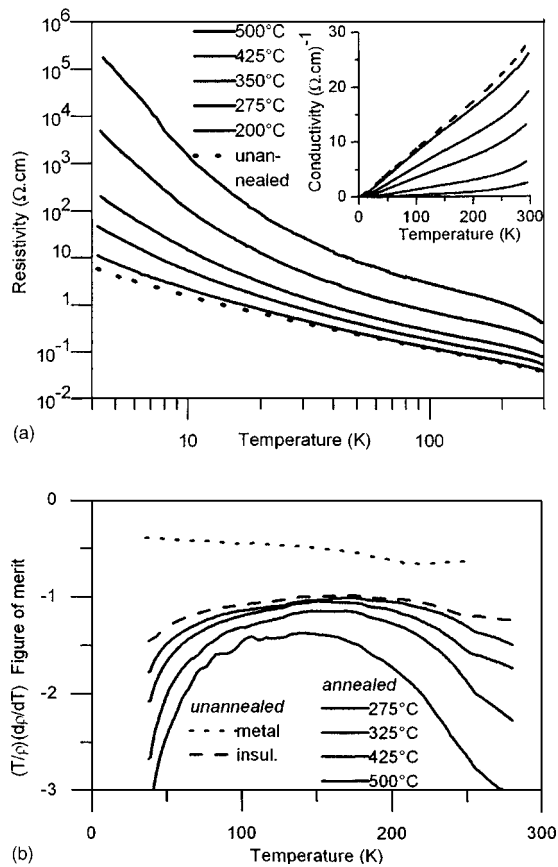


FIG. 1. (a) $\rho(T)$ on log-log scale for insulating sample (~ 8 at. %Nb) annealed at various temperatures. Dashed line: As-grown; solid lines: After annealing. Inset: Same data plotted as $\sigma (=1/\rho)$ vs T . (b) FOM $(T/\rho) \times (d\rho/dT)$ vs T for this sample unannealed and on annealing and for metallic composition (13 at. %Nb) unannealed.

and the sample annealed at 100 or 200 °C are metallic (finite conductivity when extrapolated to $T=0$ K). The sample annealed at 300 °C is very close to the MIT, and samples annealed at 400 °C and 500 °C are clearly insulating, showing that a metal-to-insulator transition can be induced by annealing.

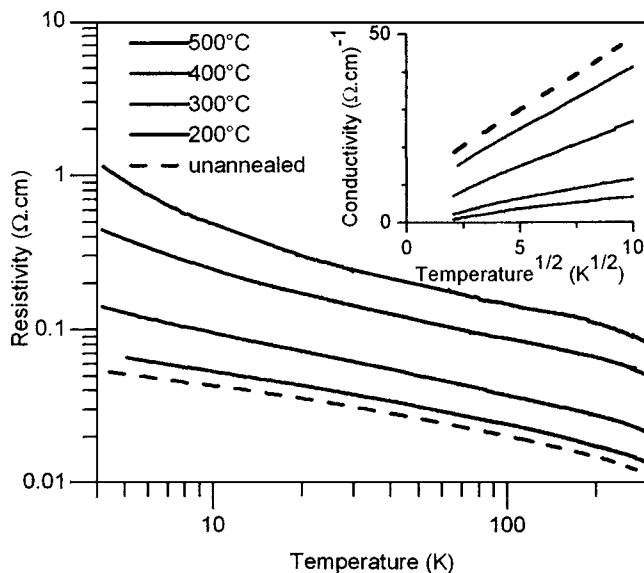


FIG. 2. (a) $\rho(T)$ of initially metallic (13 at. %Nb) sample after annealing at various T . Inset: Same data shown as σ vs $T^{1/2}$.

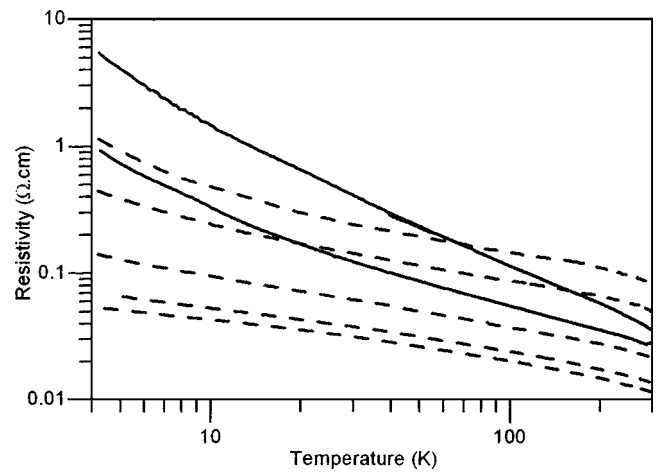


FIG. 3. Comparison of data from Fig. 2 (dotted lines) with $\rho(T)$ of as-grown $a\text{-Nb}_x\text{Si}_{1-x}$ for $x \sim 8$ and ~ 10 at. % Nb (solid lines).

This annealing-induced transition gives a family of $\rho(T)$ curves which are different from the MIT induced by changes in Nb concentration; a comparison is shown in Fig. 3. Curves of different composition spread apart on a log $\rho(T)$ scale, whereas the annealed samples shift approximately parallel to each other [Figs. 1(a) and 2]. The difference is not surprising; annealing produces an inhomogeneous sample where classical percolation plays a crucial role. The parallel shifts on a log scale suggest that annealing produces a geometric change in conduction path, an interpretation consistent with structural measurements described below.

Once a sample has been annealed for even the short time of the RTA treatment, we find that its resistivity is unaffected by subsequent heating to any temperature equal or less. This result is not surprising: Standard models for annealing-induced relaxation of the amorphous phase (with a flat distribution of diffusion barrier heights) show log time but exponential temperature dependence.^{11,12} As a result, once an amorphous sample has been exposed for even a few minutes at a given temperature, it requires extremely long times (approaching the lifetime of the universe) at the same or lower temperature for additional significant change to occur.

Annealing has several effects (both structural and chemical) on amorphous samples.¹³ We have used high-resolution cross-section transmission electron microscopy (XTEM) to understand the microscopic changes that cause the resistivity changes. The electron micrograph of an unannealed sample [Fig. 4(a)] shows the sample to be amorphous. Figures 4(b) and 4(c) show similar samples after annealing at 200 °C and 500 °C. The sample annealed at 200 °C is still amorphous and looks similar to the unannealed sample. The sample annealed at 500 °C is still predominantly amorphous, but shows the development of very small packets of lattice fringes, evidence of crystalline precursors.

We used energy-dispersive x-ray (EDX) analysis to measure compositional variations. Figure 5(a) shows the annular-dark-field (ADF) image recorded using electrons scattered to large angles as a small nanoprobe was scanned across the sample annealed at 500 °C. Bright regions of an ADF image (examples marked 1, 2, and 3) correspond to material of higher atomic number, i.e., Nb-rich areas of the sample, as verified by EDX line profiles shown in Fig. 5(b).

XTEM and ADF images show that Nb has an increasing tendency to cluster within the amorphous matrix as anneal-

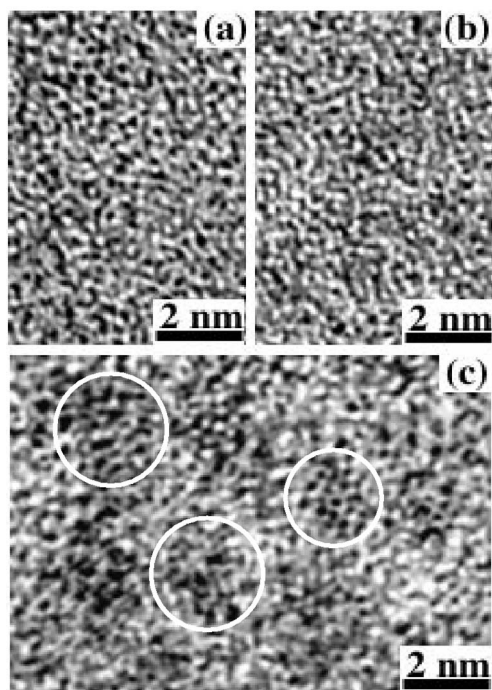


FIG. 4. High magnification XTEM of *a*-Nb-Si (~10 at. %Nb) (a) unannealed, and after annealing at: (b) 200 °C, and (c) 500 °C. Circles show examples of clusters of fringes.

ing temperature is increased. The different $\rho(T)$ shown in Fig. 3 for unannealed samples with low Nb content, and annealed samples with higher Nb content, can be explained by this observation. As Nb-rich clusters form with increasing annealing temperature, the clusters are far apart, eliminating tunneling between clusters as a significant contribution to conduction. The regions near the Nb-rich clusters are depleted of Nb, causing their resistivity to dramatically increase, and also eliminating them from significantly contributing to conduction. Therefore, conduction occurs via ever smaller regions of the sample away from the clusters with the original Nb concentration, causing ρ and $d\rho/dT$ to increase approximately proportionally (hence, approximately parallel on a log scale) as the path is increasingly restricted with increasing annealing temperature. (The proportionality is not precise, as shown by the changing FOM; it is remarkable that it is even approximately proportional, given the complexity of conduction in the clustered annealed material and the number of decades in ρ that are involved.)

These results suggest technical advances in the control of low-temperature thermometers. The extraordinary sensitivity of *a*-Nb-Si to composition makes the precise control of resistance difficult to achieve. Our results show that it is possible to deliberately make the thermometer slightly Nb rich of the desired value, and then reach the desired $\rho(T)$ by a suitable choice of annealing temperature. This approach is far easier than obtaining composition control to within fractions of an atomic %. Furthermore, annealing can be used to stabilize the thermometer against subsequent thermal degradation, allowing the chip on which the thermometer has been prepared to be exposed to temperatures well above room temperature without compromising its low-temperature properties.

In summary, we have presented the dramatic effects of annealing on amorphous $\text{Nb}_x\text{Si}_{1-x}$ films for compositions near $x=0.1$. Annealing systematically increases both ρ and

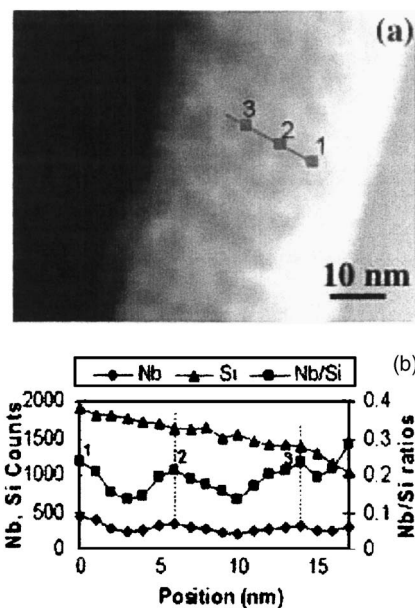


FIG. 5. (a) ADF image of *a*-Nb-Si annealed at 500 °C (b) EDX spectrum profiles showing Nb, Si, and Nb/Si ratios at positions along the line shown in (a). Values for Nb/Si ratios are significant; separate numbers are affected by varying thickness. Positions 1, 2, and 3 are shown in (a) and noted in (b); bright spots in ADF image are regions of higher than average Nb concentration.

$d\rho/dT$, and can be used to drive a transition from metal-to-insulator, starting with metallic samples close to the MIT. Annealing leads to improvements in the technological use of *a*-NbSi thermometers, specifically a more easily controlled means to produce a desired $\rho(T)$, and a way to produce a low-temperature thermometer which can withstand thermal cycling to high T . The FOM is improved by annealing, but is also strongly influenced by the initial composition. Structural analysis shows that the effect of annealing is to cause Nb to cluster within an amorphous Si-rich matrix, explaining the observed changes in $\rho(T)$.

The authors thank M. Wong for assistance, NSF-DMR and DOE for support, the Magistere Interuniversitaire de Physique for support of one of the authors (D.Q.), and gratefully acknowledge use of facilities in the John M. Cowley Center for High-Resolution Electron Microscopy at Arizona State University.

¹G. Hertel, D. J. Bishop, E. G. Spencer, J. M. Rowell, and R. C. Dynes, *Phys. Rev. Lett.* **50**, 743 (1983).

²D. J. Bishop, E. G. Spencer, and R. C. Dynes, *Solid-State Electron.* **28**, 73 (1985).

³E. Helgren, G. Gruner, M. R. Ciofalo, D. V. Baxter, and J. P. Carini, *Phys. Rev. Lett.* **87**, 116602 (2001).

⁴P. A. Lee and T. V. Ramakrishnan, *Rev. Mod. Phys.* **57**, 287 (1985).

⁵L. Dumoulin, L. Berge, H. Bernas, and M. Chapellier, *J. Low Temp. Phys.* **93**, 301 (1993).

⁶L. Dumoulin, L. Berge, S. Manieros, and J. Lesueur, *Nucl. Instrum. Methods Phys. Res. A* **370**, 211 (1996).

⁷P. Camus, L. Berge, L. Dumoulin, S. Manieros, and J. P. Torre, *Nucl. Instrum. Methods Phys. Res. A* **444**, 419 (2000).

⁸D. W. Denlinger, E. N. Abarra, K. Allen, P. W. Rooney, S. K. Watson, and F. Hellman, *Rev. Sci. Instrum.* **65**, 946 (1994).

⁹B. L. Zink, D. Revaz, R. Sappey, and F. Hellman, *Rev. Sci. Instrum.* **73**, 1841 (2002).

¹⁰B. W. Dodson, W. L. McMillan, J. M. Mochel, and R. C. Dynes, *Phys. Rev. Lett.* **46**, 46 (1981); J. Mochel (private communication).

¹¹H. Kronmuller, *Philos. Mag. B* **48**, 127 (1983).

¹²G. Hygate and M. R. J. Gibbs, *J. Phys. F: Met. Phys.* **17**, 815 (1987).

¹³T. Egami, *Mater. Res. Bull.* **13**, 557 (1978).